

Structural Evaluation and Photocatalytic Performance of Chemically Synthesised ZnO Nanoparticles

BANAJIT MALAKAR, ABU TALEB MIAH,
CHINMOY KALITA and PRANJAL SAIKIA*

Department of Applied Sciences (Chemical Science Division), Gauhati University Institute of Science and Technology, Guwahati-781014, Assam, India

psjorhat@gmail.com

Received 11 April 2015 / Accepted 18 May 2015

Abstract: This paper presents the achievability of removal of basic dye methylene blue (MB) from aqueous solutions by using homogeneous ZnO nanoparticles prepared by a very feasible modified chemical route. The prepared nanomaterial was characterized by Thermogravimetry, X-ray diffraction, Photoluminescence, FT-Infra Red and UV-Vis Spectroscopy, and Transmission Electron Microscopy analyses. The morphology of the nanoparticles were found to be very homogeneous with particle size of around 20 nm. The dye degradation was monitored with UV-Vis Spectrophotometer and the photodegradation phenomenon followed pseudo first order kinetics.

Keywords: Nanomaterials, Characterization, Photocatalysis, Chemical Synthesis, Dye degradation

Introduction

With the increasing health concern, in recent years, there has been a tremendous growth in research to find out effective measures for the removal of hazardous materials such as dyes and organic compounds from waste water^{1,2}. In this regard, nano Zinc oxide (ZnO) is emerging as a promising photocatalyst due of its high catalytic efficiency, inexpensiveness and non-toxicity³. Infact, semiconductor metal oxide nanomaterials have attracted much more attention due to their utility not only as efficient electron mediators for the photocatalytic degradation⁴ but also their applications in gas sensors,⁵ lithium storage⁶ and water-splitting⁷. ZnO is an n-type semiconductor with wide and direct bandgap ($E_g = 3.37$ eV at room temperature), high exciton binding or Rydberg energy (60 meV at room temperature), unique optical and luminescence properties^{8,9}. Due to the presence of oxygen vacancies that in turn impart superior conducting properties, nanostructured ZnO can be utilized efficiently as a photocatalyst towards degradation of organic dye pollutant^{10,11}. Moreover, it has high quantum efficiency, high redox potential, advanced physical and chemical stability¹². Semiconductors upon illumination with solar or UV light source, produces electron/hole pairs, where electrons are promoted to the conduction band leaving behind positive holes in the valence band. In presence of surface oxygen vacancies, the

generated electron/hole pairs could initiate a series of reactions by reacting with surface bound hydroxyl groups (OH) or O₂ from water resulting in the formation reactive radicals like O₂^{•-}, OH[•] that significantly contribute in the complete degradation of organic pollutants in water¹³.

As size and shape dependence is a very crucial property of nanomaterials, various methods have been employed for the synthesis of ZnO nanostructures with different shapes and properties¹⁴. Based on shape, numerous ZnO nanostructures have been reported, such as nanoparticles¹⁵, nanorods¹⁶, nanocombs¹⁷, nanowires¹⁸, nanotubes¹⁹, nanoflowers²⁰, *etc.* Among these, ZnO nanoparticle with the presence of oxygen vacancy can effectively reduce Methylene Blue (MB) dye in water²¹. MB, also known with the chemical name tetramethylthionine chloride, was the first synthetic drug used in medicine and was used for the treatment of malaria^{22,23}. It is a phenothiazine cationic dye and a monoamine oxidase inhibitor (MAOI)²⁴. Infusion of MB at doses exceeding 5 mg/kg results in combination of MB with any selective serotonin reuptake inhibitors like duloxetine, sibutramine, venlafaxine, clomipramine, imipramine and may precipitate serious serotonin toxicity, serotonin syndrome²⁵. It affects the 5-hydroxytryptamine system and causes dizziness, headache, tremors, seizures and mental confusion^{26,27}. Noteworthy that MB is hard to degrade. Therefore, degradation of MB in water do deserves serious attention.

In the present work, we report an economical and facile route for the synthesis of ZnO nanoparticle. This method uses low-temperature and avoids harsh reaction condition. Another aspect of the present study is to evaluate the photocatalytic activity of the ZnO nanoparticles for waste water treatment.

Experimental

Zinc acetate dihydrate was purchased from Sigma Aldrich with the purity of 98 wt% and was used as precursor. Ethanol and sodium hydroxide pellets were purchased Merck. Analytical reagent methylene Blue dye was supplied by HiMedia. All the chemicals were used as purchased without further purification. Deionised distilled water obtained from Millipore system was used in the preparation of solutions.

Preparation of ZnO nanoparticles

ZnO nanoparticles materials were prepared by direct precipitation method described by *Borghesi et al.*,¹⁵ with some modifications. In a typical synthetic procedure, solution of equal volume of Zinc acetate dihydrate and sodium hydroxide were prepared separately in distilled deionized water at a ratio of the concentrations 1:2 (zinc acetate dehydrate : sodium hydroxide). Then the synthesis was carried out by drop-wise addition of sodium hydroxide solution to the zinc acetate dihydrate solution under vigorous stirring at room temperature, to form a transparent white solution. The solution mixture was allowed to react for 5 hours so as to slowly produce the ZnO particles. The precipitates obtained from the reaction mixture is collected and washed with distilled deionized water and then with ethanol several times using centrifugation. The washed precipitates were dried in an electric oven at 100 °C, by keeping it overnight to form ZnO precursor. Following this, the precursors were calcinated at 400 °C for 4 h to form ZnO nanoparticle.

Preparation of reaction set-up for photocatalytic degradation of methylene blue using ZnO nanoparticle

In this study, degradation of 30 mL of 10 ppm methylene blue (MB) dye solution at 120 minutes was investigated using the 0.2g L⁻¹ of as-synthesized ZnO nanoparticle. The MB dye solution and catalyst was taken in a round bottom flux. To establish the adsorption

equilibrium between the dye molecules and the catalyst surface, the mixture was stirred in dark for 20 minutes. The solution was then irradiated with solar light. The decolourization efficiency (%) was calculated as follows:

$$\% \text{ Degradation} = [(A_0 - A_t) / A_0] \times 100$$

Where A_0 is the initial absorbance of dye and A_t is the absorbance of dye at time 't' after photo-irradiation. The photocatalytic reduction reaction was carried out for 120 min as no further degradation was observed after that. The catalyst was recovered by centrifugation to study the effectiveness of the recovered catalyst. The reaction was studied under solar light in summer season between 11 AM and 3 PM during which fluctuation of solar intensity is minimum²⁸.

Characterization of materials

The powder X-ray diffraction (XRD) patterns were recorded on a Rigaku Multiflex instrument for 2θ values from $10-80^\circ$ using nickel-filtered $\text{CuK}\alpha$ (0.15418 nm) radiation source and a scintillation counter detector. Thermogravimetric analysis was done using a Mettler Toledo TG-SDTA instrument where the samples were heated up to 1000°C at a heating rate of $10^\circ\text{C}/\text{min}$. Infra-red spectra were measured using a FT-IR spectrophotometer, Model Spectrum Two FT-IR Spectrometer (Perkin Elmer). Measurements were achieved by pelletizing the samples with KBr in the mid-infrared region at an accelerating voltage of 200 V. Transmission Electron Micrographs (TEM) were captured with JEOL JEM 2100 TEM instrument operated at 200 kV. UV-spectrums were recorded using UV-Vis spectrophotometer (Model-Perkin Elmer Lambda 35). Photoluminescence (PL) spectra were recorded by Hitachi F-2500, fluorescence spectrometer.

Results and Discussion

XRD analysis

Figure 1 represents XRD pattern of synthesized ZnO nanoparticle. The XRD pattern shows diffraction peaks at $2\theta = 31.6^\circ, 34.2^\circ, 36.1^\circ, 47.3^\circ, 56.3^\circ, 62.7^\circ, 66.2^\circ, 67.5^\circ, 68.8^\circ, 72.4^\circ$ and 77.2° belong to the (100), (002), (101), (102), (110), (103), (200), (201), (004) and (202) planes respectively, which corresponds to the hexagonal wurtzite structure of ZnO (JCPDS No. 36-1451)²⁹.

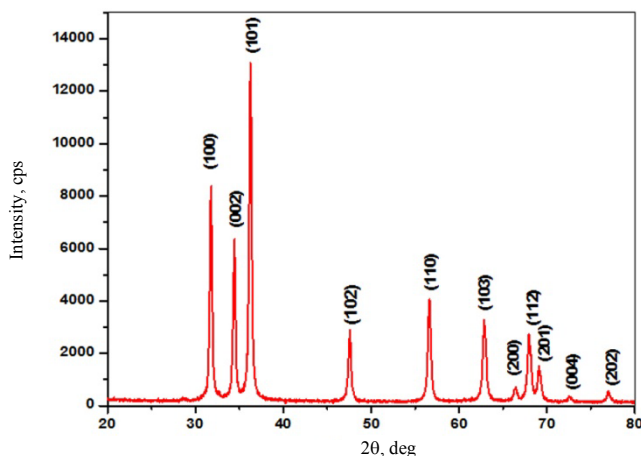


Figure 1. X-Ray diffraction pattern of ZnO nanoparticle

In the XRD analysis, no prominent peak for any other phase was found, which reveals the high purity of the synthesized product.

TG analysis

Thermal stability of the synthesised material was investigated with the help of thermogravimetric analysis. The temperature suitable for calcinations of the sample could be chosen on the basis of this analysis. The temperature at which mass loss was stabilised was regarded as the suitable calcinations temperature. As presented in Figure 2, three distinct mass loss features are observed. One feature at around 80-100 °C was due to the loss of molecularly adsorbed water from surface. Another weight loss feature in the range 150-220 °C could be primarily due to the loss of nondissociative adsorbed water as well as water held on the surface by hydrogen bonding. The sample exhibited one major weight loss peak in the range 250-400 °C due to the loss impurities from the bulk. Above that, no further weight loss was observed. Therefore, the calcinations temperature for the sample was chosen to be 400 °C. The stabilization in weight loss after 400 °C implies that Zinc hydroxides are completely converted to ZnO nanoparticles after calcination. Moreover, it could be inferred that the synthesized ZnO nanoparticles are thermally quite stable at high temperatures (up to 1000 °C)³⁰.

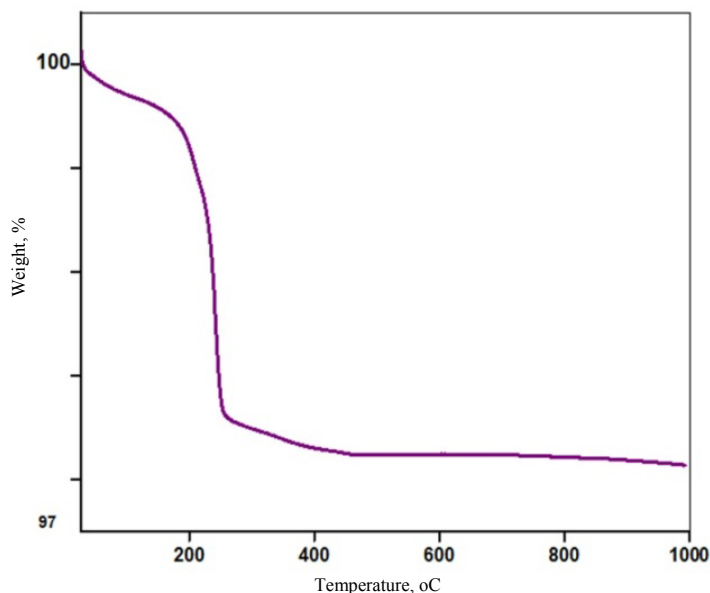


Figure 2. TGA profile of ZnO nanoparticle

FT-IR analysis

Fourier Transform Infrared spectra of Zinc oxide nanoparticles were recorded in the frequency range 400-4000 cm^{-1} by preparing KBr pellet and operating at a resolution of 4 cm^{-1} . The FT-IR spectra for ZnO nanoparticles is shown in Figure 3. A strong band at $\sim 3446 \text{ cm}^{-1}$ is due to surface adsorbed O-H stretching mode of vibration in ZnO nanoparticle and the characteristic stretching band for Zn-O is observed at $\sim 439 \text{ cm}^{-1}$. The peaks at $\sim 1650 \text{ cm}^{-1}$ may be due to the presence of water molecules in KBr, which is used in the preparation of sample for FT-IR analysis³¹.

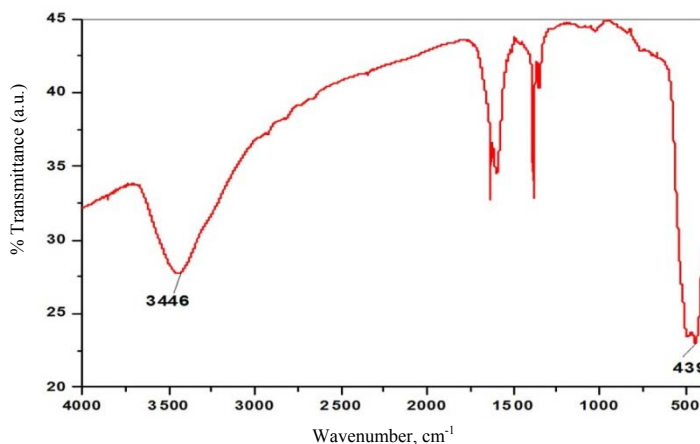


Figure 3. FT-IR spectra of ZnO nanoparticle

TEM analysis

The HRTEM image of ZnO nanoparticle is shown in Figure 4. The particle sizes are in the range of 20 nm and imply that the shapes are almost spherical in nature (Figure 4a and 4b). The particles are homogeneous in nature which would be crucial for showing better catalytic activity. The selected area electron diffraction (SAED, Figure 4a) reveals the good crystalline nature of the material. The measured lattice spacing from HRTEM micrograph (Figure 4c) was found to be 0.30 nm corresponding to the (100) plane of hexagonal ZnO³².

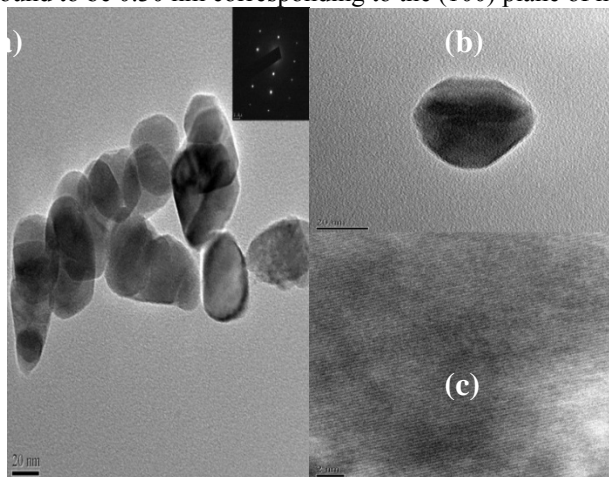


Figure 4. TEM image of (a) as prepared ZnO, (b) single ZnO nanoparticle, (c) HRTEM image for ZnO

PL analysis

Figure 5 shows the Photoluminescence (PL) emission from the prepared ZnO nanoparticles dispersed in double distilled water. The ZnO nanoparticle shows an ultraviolet (UV) emission at about 390 nm and defect related band within 480-700 nm range. Moreover, a minor peak at 445 nm (blue) and a strong maximum major peak at ~565 nm (green wavelength) are observed. UV emission originates from the free exciton recombination related

to near-band-edge (NBE) emission. Reports suggest that generally the proposed visible emissions are associated with deep level (DL) defect(s) causing the emission. Color from ZnO film are mainly due to the intrinsic defects such as oxygen vacancies (V_O), zinc vacancies (V_{Zn}), interstitial oxygen (O_i), interstitial zinc (Zn_i), antisite oxygen (O_{Zn}) and antisite zinc (Zn_O). The weak and broad blue emission band at ~ 468 nm is due to the DL transition from Zn_i to V_{Zn} or Conduction Band (CB) to V_{Zn} , whereas green emission band at ~ 565 nm is possibly due to the DL transition^{33,34} from CB to V_O , or to V_{Zn} , or C.B. to both V_O and V_{Zn} .

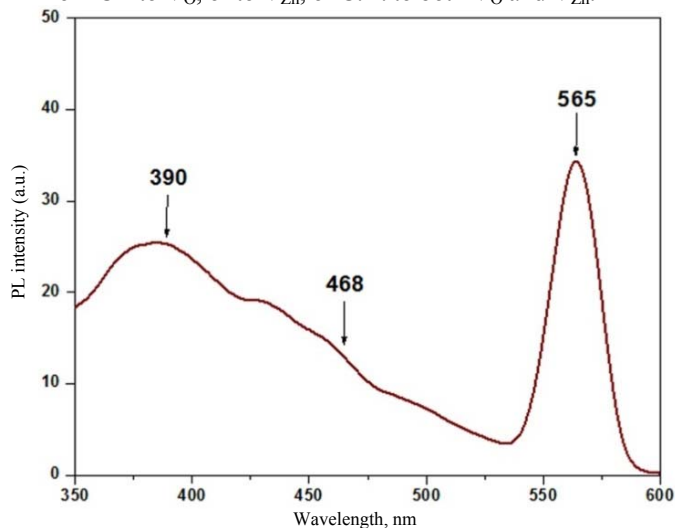


Figure 5. Room temperature PL spectra of ZnO nanoparticle

UV-Visible spectral analysis ZnO nanoparticle

The formation of Zinc oxide nanoparticle was studied by analysing it with UV-Visible Spectrophotometer in the range of 200-700 nm. Figure 6 shows the characteristic peak at ~ 372 nm for ZnO nanoparticle³⁵. The band gap value calculated from the spectrum was found to be ~ 3.33 eV that reinforces the semiconducting property of the material.

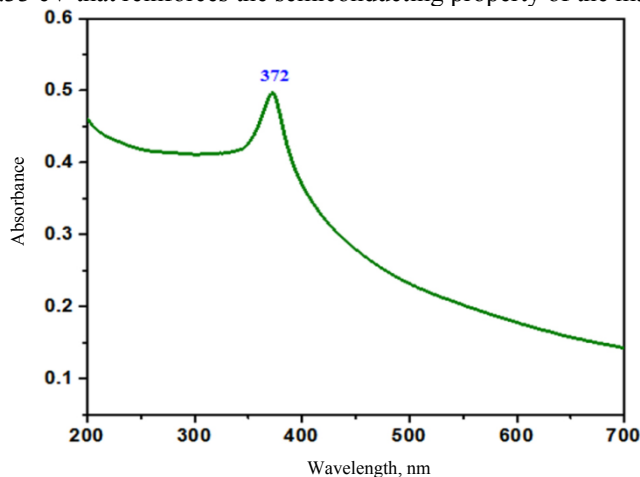
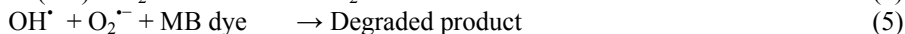
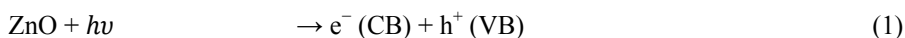


Figure 6. UV spectra of ZnO nanoparticle

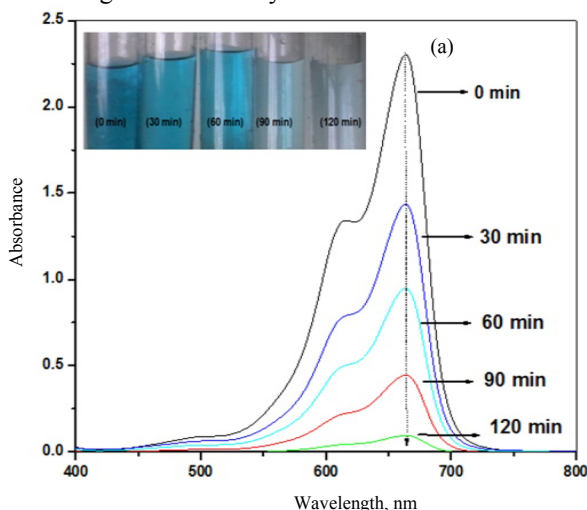
Photocatalytic degradation of methylene Blue using ZnO nanoparticle mechanism

The solar light induced photocatalytic activity of the synthesized ZnO is due to the electron promotion from the valance band to the conduction band of the semiconducting oxide resulting generation of electron-hole pairs as shown in equation (1). The valance band hole h^+ (VB) is a region of positive charge which react with adsorbed water molecules and surface-bound hydroxyl groups (OH^-) to generate hydroxyl radicals (OH^\bullet) as shown in equations (2) and (3). The conduction band electron e^- (CB) is a region of negative charge that reduces the oxygen molecules present in the solution by forming a superoxide radical anion ($O_2^{\bullet-}$) as in equation (4). Hydroxyl radicals are known to be powerful oxidizing agents ($E_o = +3.06$ V)³⁶. During the photocatalytic process, MB was believed to be degraded through direct oxidation by the OH^\bullet radicals and $O_2^{\bullet-}$ radicals as shown in equation (5)³⁷. The possible reaction mechanism for photocatalytic degradation of MB dye using zinc oxide nanoparticle can be describe as follows:



Activity study

To study the photocatalytic activity of ZnO nanoparticle under solar light source, experiments were carried out using 0.2g L^{-1} of synthesized ZnO nanoparticle and 30 mL of 10 ppm MB dye with stirring time of 120 minutes. Figure 7a shows the UV-visible absorption spectra of 10 ppm MB aqueous solutions with ZnO photocatalyst following the irradiation with sun light for different durations of time. The characteristic absorption peak of MB at 662 nm is monitored as a function of sunlight exposure time and degradation of MB is studied at this particular characteristic peak using UV-spectrophotometer. As shown in inset of Figure 7a, the colour of MB dye changes from blue to colourless upon complete degradation. Figure 7b shows degradation percentage of MB dye at different time interval. From Figure 7, degradation percentage of MB dye is calculated and found to be 96.16% in 120 minute. No further degradation MB dye was achieved after 120 minute.



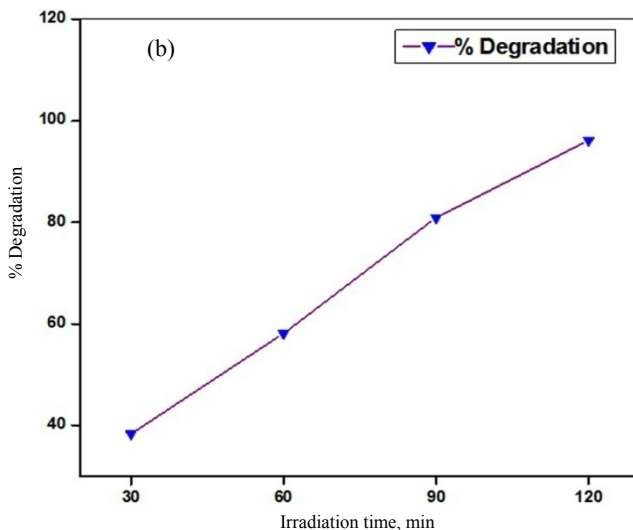
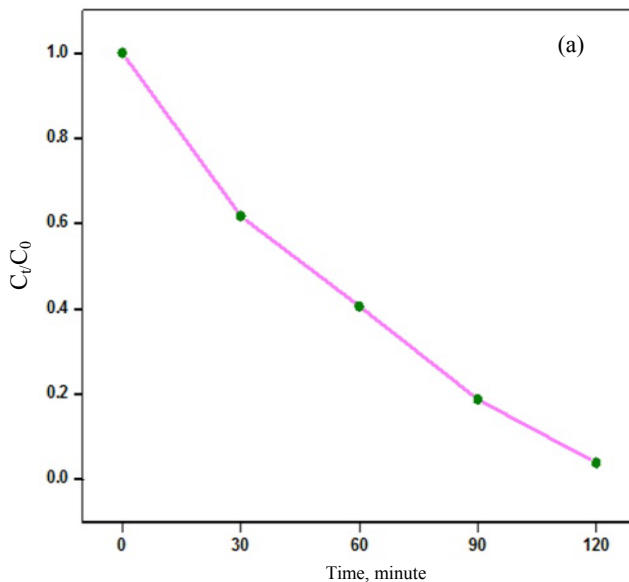


Figure 7. (a) UV spectra of MB dye Degradation using ZnO nanoparticle (b) % degradation of MB dye w.r.t. time

Figure 8a and 8b shows the kinetics study of MB dye degradation by using ZnO nanoparticle under solar-light exposure. To study the kinetics of the catalytic reaction the absorbance at 662 nm of the MB dye and ZnO mixed reaction solution was measured as a function of time. The plots of C_t/C_0 and $\ln(C_0/C_t)$ against the reaction time is shown in Figure 8a and 8b respectively. The C_0 and C_t in the plots of C_t/C_0 and $\ln(C_0/C_t)$ against reaction time are the concentrations of MB dye at 0 and t time, respectively. The kinetic curves for degradation of MG dye (Figure 8b) follows pseudo first order kinetics. From Figure 8b the calculated apparent rate constant, K_{app} (min^{-1}) is found to be 0.026 min^{-1} and the R^2 value is 0.957.



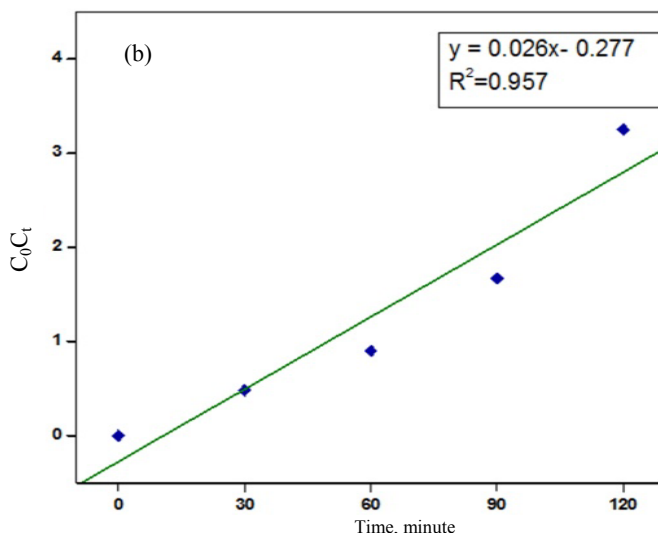


Figure 8. (a,b) Kinetics of MB photodegradation by ZnO nanoparticle w.r.t. time

Reusability analysis of ZnO nanoparticles

It can be clearly seen that the efficiency of the photocatalyst remains high even after four runs. The ZnO nanoparticles were recovered using centrifugation and washed several times with water and ethanol and then dried in an oven overnight at 100 °C. The recovered ZnO catalyst is reused for next three runs, which degrades MB with a minimal decrease in efficiency. This is possibly due to the loss of catalyst during centrifugation.

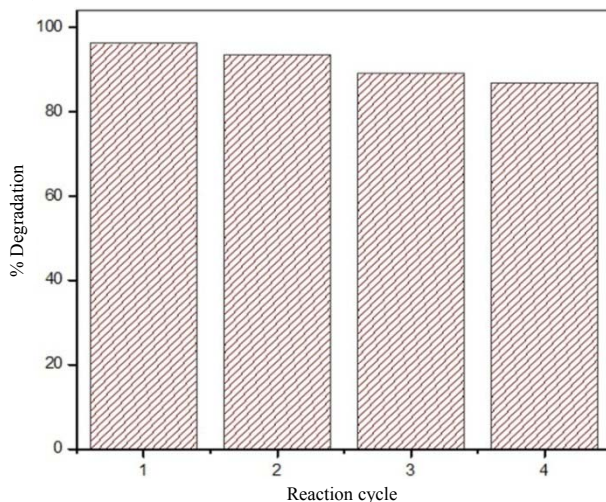


Figure 9. Reusability study of ZnO nanoparticles for photocatalytic degradation of MB dye under solar light.

Conclusion

In summary, ZnO nanoparticles have been synthesized by using a very feasible modified chemical synthesis. The structural characteristics and its application towards waste water

treatment have been systematically investigated. The formation of ZnO nanoparticles was confirmed from XRD, UV-Vis and PL analyses. Thermogravimetric analysis showed high thermal stability of the synthesised material. The TEM micrographs indicated the formation of nanosized ZnO with reasonably good homogeneity. HREM micrograph confirmed lattice spacing of 0.30 nm exposing the (100) plane of hexagonal ZnO. The synthesised material displayed significant photo-catalytic performance for MB dye degradation with superior reusability following a pseudo first order kinetics.

Acknowledgment

PS and ATM thank DST (New Delhi) for project grant No. SR/FT/CS-69/2011. Authors also thank SAIF, NEHU and USIC, Gauhati University for providing instrumental facilities.

References

- 1 Udawatte N, Lee M, Kim J and Lee D, *ACS Appl Mater Interfaces*, 2011, **3(11)**, 4531-4538; DOI:10.1021/am201221x
- 2 Chen G, Sun M, Wei Q, Zhang Y, Zhu B and Du B, *J Haz Mater.*, 2013, **244-245**, 86-93; DOI:10.1016/j.jhazmat.2012.11.032
- 3 Hong T K, Tripathy N, Son H J, Ha K T, Jeong H S and Hahn Y B, *J Mater Chem B*, 2013, **1**, 2985-2992; DOI:10.1039/C3TB20251H
- 4 Singh A K and Nakate U T, *J Nanoparticles*, 2013, **2013(310809)**, 7; DOI:10.1155/2013/310809
- 5 Hosseinia Z S, Zad A I and Mortezaalia A, *Sensors Actuators B, Chem.*, 2015, **207**, 865-871; DOI:10.1016/j.snb.2014.10.085
- 6 Bresser D, Mueller F, Fiedler M, Krueger S, Kloepsch R, Baither D, Winter M, Paillard E and Passerini S, *Chem Mater.*, 2013, **25(24)**, 4977-4985; DOI:10.1021/cm403443t
- 7 Wang T, Lv R, Zhang P, Li C and Gong J, *Nanoscale*, 2015, **7**, 77-81; DOI:10.1039/C4NR03735A
- 8 Kaur J, Kumar P, Sathiaraj T S and Thangaraj R, *Int Nano Lett.*, 2013, **3-4**; DOI:10.1186/2228-5326-3-4
- 9 Jiang D, Cao L, Liu W, Su G, Qu H, Sun Y and Dong B, *Nanoscale Res Lett.*, 2009, **4(1)**, 78-83; DOI:10.1007/s11671-008-9205-6
- 10 Lv T, Pan L, Liu X and Sun Z, *Catal Sci Technol.*, 2012, **2**, 2297-2301; DOI:10.1039/C2CY20023F
- 11 Bagabas A, Alshammari A, Aboud M F A and Kosslick H, *Nanoscale Res Lett.*, 2013, **8**, 516; DOI:10.1186/1556-276X-8-516
- 12 Wang Z L, *J Phys Condens Matter.*, 2004, **16**, 829.
- 13 Nagaraja R, Kottam N, Girija C R and Nagabhushana B M, *Powder Tech.*, 2012, **215-216**, 91-97.
- 14 Radzimska A K and Jesionowski T, *Materials*, 2014, **7(4)**, 2833-2881; DOI:10.3390/ma7042833
- 15 Moazzen M A M, Borghei S M and Taleshi F, *Appl Nanosci.*, 2013, **3(4)**, 295-302; DOI:10.1007/s13204-012-0147-z
- 16 Polsongkram D, Chamninok P, Pukird S, Chow L, Lupan O, Chai G, Khallaf H, Park S and Schulte A, *Physica B: Condensed Matter*, 2008, **403(19-20)**, 3713-3717; DOI:10.1016/j.physb.2008.06.020
- 17 Zhuo R F, Feng H T, Liang Q, Liu J Z, Chen J T, Yan D, Feng J J, Li H J, Cheng S, Geng B S, Xu X Y, Wang J, Wu Z G, Yan P X and Yue G H, *J Phys D: Appl Phys.*, 2008, **41**, 185405.

- 18 Yang P, Yan H, Mao S, Russo R, Johnson J, Saykally R, Morris N, Pham J, He R and Choi H J, *Adv Funct Mater.*, 2002, **12**, 323-331; DOI:10.1002/1616-3028(20020517)12:5<323::AID-ADFM323>3.0.CO;2-G
- 19 Tong Y, Liu Y, Shao C, Liu Y, Xu C, Zhang J, Lu Y, Shen D and Fan X, *J Phys Chem B*, 2006, **110(30)**, 14714-14718; DOI:10.1021/jp056654h
- 20 Chakraborty S, Kole A K and Kumbhakar P, *Mat Lett.*, 2012, **67(1)**, 362-364; DOI:10.1016/j.matlet.2011.10.018
- 21 Jain N, Bhargava A and Panwar J, *Chem Eng J.*, 2014, **243**, 549-555; DOI:10.1016/j.cej.2013.11.085
- 22 Guttmann P and Ehrlich P, *Berliner Klinische Wochenschrift*, 1891, **28**, 953-956.
- 23 Wainwright M and Crossley K B, *J Chemother.*, 2002, **14(5)**, 431-443.
- 24 Ramsay R R, Dunford C and Gillman P K, *Brit J Pharmacol.*, 2007, **152(6)**, 946-951; DOI:10.1038/sj.bjp.0707430
- 25 Cragan J D, *Teratology*, 1999, **60(1)**, 42-48; DOI:10.1002/(SICI)1096-9926(199907)60:1<42::AID-TERA12>3.0.CO;2-Z
- 26 Oz M, Isaev D, Lorke D E, Hasan M, Petroianu G and Shippenberg T S, *Brit J Pharmacol.*, 2012, **166(1)**, 168-176; DOI:10.1111/j.1476-5381.2011.01462.x
- 27 Khan M A, North A P and Chadwick D R, *Ann R Coll Surg Engl.*, 2007, **89(2)**, W9-11.
- 28 Tripathi A and Srivastava S K, *Int J Bioscience, Biochemistry and Bioinformatics* 2011, **1(1)**, 37-40; DOI:10.7763/IJBBB.2011.V1.7
- 29 Chena C, Yua B, Liub P, Liua J F and Wanga L, *J Ceramic Process Res.*, 2011, **12**, 420-425.
- 30 Bagheri S, Chandrappa K G and Hamid S B A, *Der Pharma Chemica*, 2013, **5(3)**, 265-270.
- 31 Viswanatha R, Venkatesh T G, Vidyasagar C C and Arch Y A N, *Appl Sci Res.*, 2012, **4(1)**, 480-486.
- 32 Bindu P and Thomas S, *J Theor Appl Phys.*, 2014, **8(4)**, 123-134.
- 33 Willander M, Nur O, Sadaf J R, Qadir M I, Zaman S, Zainelabdin A, Bano N and Hussain I, *Materials*, 2010, **3(4)**, 2643-2667; DOI:10.3390/ma3042643
- 34 Ahn C H, Kim Y Y, Kim D C, Mohanta S K and Cho H K, *J Appl Phys.*, 2009, **105(1)**, 013502; DOI:10.1063/1.3054175
- 35 Mishra S K, Srivastava R K, Prakash S G, Yadav R S and Panday A C, *Opto Electron Rev.*, 2010, **18(4)**, 467-473.
- 36 Khezrianjoo S and Revanasiddappa H D, *J Catal.*, 2013, **2013(582058)**, 1.
- 37 Pung S Y, Lee W P and Aziz A, *Int J Inorg Chem.*, 2012, **2012(608183)**, 9; DOI:10.1155/2012/608183